

Microwave accelerated facile synthesis of fused polynuclear hydrocarbons in dry media by intramolecular Friedel–Crafts alkylation

Vanya B. Kurteva,^{a,b} António Gil Santos^b and Carlos A. M. Afonso^{*b}

^a Institute of Organic Chemistry, Bulgarian Academy of Sciences, Acad. G. Bonchev str., Block 9, 1113 Sofia, Bulgaria

^b REQUIMTE/CQFB, Departamento de Química, Faculdade de Ciências e Tecnologia, Universidade Nova de Lisboa, 2829-516 Caparica, Portugal.

E-mail: cma@dq.fct.unl.pt; for modelling aspects; ags@dq.fct.unl.pt; Fax: + 351 21 2948550; Tel: + 351 21 2948358

Received 23rd September 2003, Accepted 10th December 2003
First published as an Advance Article on the web 21st January 2004

Fused polynuclear tetrahydro arenes are synthesised in a fast, simple, high yielding and regioselective procedure by an intramolecular Friedel–Crafts alkylation in dry media under microwave irradiation of the corresponding 1-bromo-4-arylbutanes immobilised on silica. The observed reactivity is rationalised by molecular modelling studies which suggest the occurrence of a concerted mechanism.

Introduction

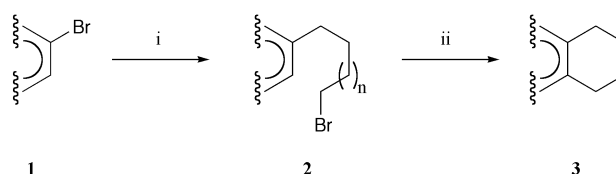
Organic reactions performed under microwave irradiation (MWI) have some significant advantages in comparison with the conventionally heated ones, such as much shorter reaction times, better selectivities and higher yields.¹ The use of a clean, efficient and economical solvent-free procedure combined with an immobilisation on solid support reagents technique, which gives good dispersion of the active reagent sites, associated selectivity and easier work-up,² is an environmentally benign procedure preventing release of reaction residues into the environment.

Polynuclear hydroaromatic hydrocarbons are well known and widely investigated compounds.^{3a} They have been synthesised mainly by partial hydrogenation of polycyclic arenes, as complicated mixtures of regioisomers of products with different degrees of hydrogenation. Other methods included the intramolecular Friedel–Crafts acylation followed by carbonyl reduction.^{3b–c} On the other hand, the reported examples of intramolecular Friedel–Crafts alkylation have been mainly restricted to benzene and naphthalene.^{3d–i} Additionally, some photochemically irradiated transformations of arylbromoalkanes have been reported on the model of phenylbromobutane, where the cyclisation product, tetrahydronaphthalene, has been isolated in less than 20%, parallel with reduction and elimination products.⁴

In the course of our attempt to prepare the 4-(9-phenanthrenyl)butyl acrylic ester by nucleophilic substitution of the corresponding alkyl bromide **2a** with acrylic acid on a silica gel support, assisted by a microwave (MW),⁵ we observed instead the exclusive formation of the polynuclear hydrocarbon **3a** in high yield (91%). With such unexpected result in hand, we studied this transformation in more detail. Herein we report a simple, high yield and regioselective synthesis of polycyclic hydrocarbons from the corresponding aryl alkyl bromides, using solid-supported reagents, in a microwave accelerated solventless procedure (Scheme 1), with the reactivity being rationalised by molecular modelling.

Results and discussion

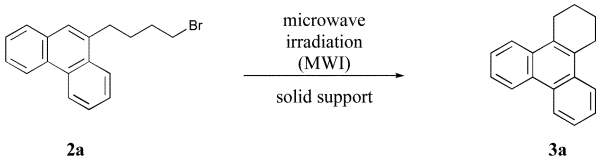
The starting 1-bromo-*n*-arylalkanes **2** were prepared from the corresponding aryl bromide **1**, by lithium–bromide exchange



Scheme 1 General method used for the preparation of fused polynuclear hydrocarbons **3**. i) *n*-BuLi (1.5 eq.), diethyl ether; α,ω -dibromoalkane (4 eq.); ii) silica gel (2 g per mmol of bromide **2**), MWI (800 W), 15 min.

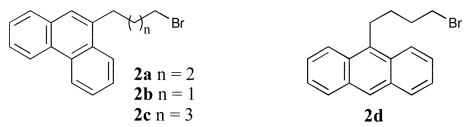
followed by reaction with an excess of α,ω -dibromoalkane using standard conditions.⁶

The bromides **2** were impregnated onto the silica gel support by prior preparation of dichloromethane solutions followed by subsequent solvent removal, and then were submitted to microwave irradiation in a domestic household oven (“dry media” conditions). Initially, this transformation was studied under different experimental conditions using 1-bromo-4-(9-phenanthrenyl)butane **2a** as a substrate model (Table 1). An increase in the MW power gives higher conversion (entry 1, 600 W, 15% vs entry 7, 800 W, 82% and entry 4, 700 W, 61% vs entry 8, 800 W, 94%) and no reaction was observed when using basic alumina, instead of silica (entry 1 vs entry 2). We also studied the effect of several additives immobilised on the silica support: while the basic salts K_2CO_3 or AcONa gave a considerable reduction on the conversion (entry 11, 46% and entry 12, 50% vs entry 8, 94%), the acid CF_3CO_2H originated only a small reduction on the conversion (entry 13, 89%). On the other hand, the radical inhibitor BHT as well as hexabutyliditin also effected a considerable reduction on the conversion (entry 9, 71% and entry 10, 63% vs entry 8, 94%). In contrast to the high conversion using MWI on substrate **2a** (Table 1, entry 8, 94%), no reaction was observed by submitting the bromide **2a** to vigorous thermal conditions (138 °C, 6 h, Table 2, entry 1), or on the attempt to effect the intermolecular assisted MW Friedel–Crafts alkylation of phenanthrene with 1,4-dibromobutane (Table 2, entry 5). Interestingly, no reaction was observed for the substrates **2b** and **2c** containing the propane and pentane alkyl chains, respectively, or for substrate **2d** (Table 2, entries 2–4) which is in contrast to the high conversion observed for the butane alkyl chain **2a** under similar experimental conditions (Table 1, entry 8). In the case of ester **4**

Table 1 Conversion of **2a** into **3a** under different experimental conditions^a


Entry	Power/W	Time/min	Solid support	Additive ^b	Conv. ^c (%)
1	600	10	Silica	No	15
2	600	10	Basic alumina	No	None ^f
3	600	10	Basic alumina	K ₂ CO ₃	None ^f
4	700	15	Silica	No	61
5	700	15	Silica	MeCO ₂ Na	71
6	700	15	Silica	Aliquat [®] 336 ^d	56
7	800	10	Silica	No	82
8	800	15	Silica	No	94
9	800	15	Silica	BHT ^e	71
10	800	15	Silica	(<i>n</i> -Bu ₃ Sn) ₂	63
11	800	15	Silica	K ₂ CO ₃	46
12	800	15	Silica	MeCO ₂ Na	50
13	800	15	Silica	CF ₃ CO ₂ H	89

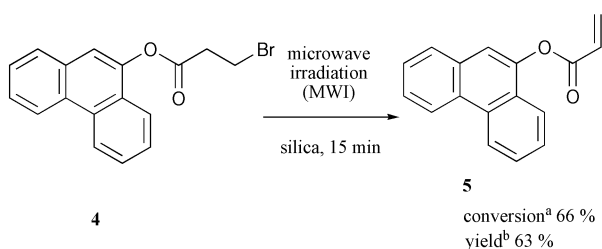
^a The position of the reaction flask in the microwave oven was prior optimised and fixed for all the examples presented here. In all experiments were used 2.0 g of solid support/mmol of bromide **2a**. ^b When applied, was used 1.0 mol eq. of additive. ^c Observed conversion by ¹H NMR. ^d Aliquat[®] 336 (tricaprylmethylammonium chloride). ^e BHT (2,6-di-*t*-butyl-4-methylphenol). ^f None of the product **3a** was detected by TLC and by ¹H NMR.

Table 2 Attempts to effect the Friedel–Crafts alkylation


Entry	Substrate	Conditions	Result
1	2a	Xylene, reflux, 6 h	Starting material ^d
2	2b	MW, 800 W, 75 min	Starting material ^d
3	2c	MW, 800 W, 75 min	Starting material ^d
4	2d	MW, 800 W, 30 min	Starting material ^d
5	Phenanthrene	1,4-Dibromobutane, MW, 800 W, 15 min	Starting material ^d

^a No reaction was observed by TLC and ¹H NMR.

no formation of the desired cyclised product was observed, giving instead the corresponding acrylate **5** in moderate yield (Scheme 2).



Scheme 2 Attempt to effect the Friedel–Crafts alkylation on the ester **4**. ^a Observed conversion by ¹H NMR. ^b Isolated yield after purification by flash chromatography.

The scope of this transformation was further evaluated for different substrates under optimised conditions (Table 3). The proposed structures of the fused aromatic hydrocarbons were based on comparisons with reported spectral and analytical data and were confirmed by 2D NMR (COSY, NOESY and HMQC). In fact, for the correct assignment of the non-equivalent benzylic ethylene protons and the aromatic protons, which show the place of annulation, the NOESY cross peaks are of great importance.

The investigated microwave accelerated cyclisation proceeds regioselectively *via* substitution of the aromatic proton

neighbouring the alkyl side chain, in all substrates tested, which is in an accordance with the lack of reactivity of the 9-anthracenyl bromobutane **2d** under the same conditions.

The transformation occurred in high yields 72–97% (Table 3) when fused polynuclear aromatic hydrocarbons were formed (**3a**, **3e–3h**) while low yields were found for 1,2,3,4-tetrahydronaphthalene **3i** (13%) and 5-phenyl-1,2,3,4-tetrahydronaphthalene **3k** (14%), where the aromatic substituents in the starting bromides were of a simple phenyl type. In contrast, complete conversion of **2j** to **3j** was observed. Interestingly, the substrate **2g** gives only the isomer **3f**. These results suggest that this transformation is strongly dependent on the aromatic ring structure and the size of the alkyl chain. This reaction is applicable as a high yield procedure for the synthesis of fused aromatic hydrocarbons, if the annulating center is activated by an alkyl or aryl substituent in the *ortho* position. It should also be mentioned that in all substrates tested the transformation is very clean, without any traces of other products apart from recovered starting material **2** and product **3**.

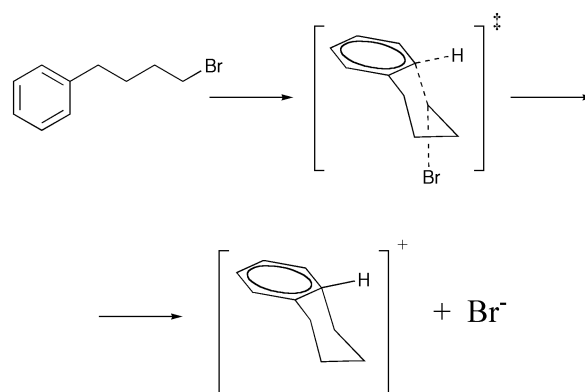
The liberation of hydrogen bromide from this reaction is an important issue from a synthetic and environmental point of view. However, we observed that the by-product of the reaction, hydrogen bromide, is well adsorbed on silica gel (above 70%). The residual content of HBr on silica was determined by titration with aqueous NaOH solution of an aqueous suspension of both the crude reaction mixture and the silica gel, after extraction of the organic products with dichloromethane.

Table 3 MW assisted cyclisations of 4-aryl-1-bromobutanes **2**^a

	Substrate 2	Product 3	Conversion (%) ^b	Yield (%) ^c
a			95	91
e			Complete	97
f			94	91
g		3f	Complete	96
h			76	72
i			17	13
j			Complete	96
k			19	14

^a Silica gel (2 g per mmol of bromide **2**), MW irradiation (800 W), 15 min. ^b Observed conversion by ¹H NMR. ^c Isolated yield after purification by flash chromatography.

The photochemistry of alkyl bromides and iodides, including 1-bromo and 1-iodo-phenylbutane, have been studied in detail, where it is assumed that, in general, the reaction occurs *via* formation of radical and carbocation reactive intermediates, respectively for iodides and bromides.⁴ Additionally, for the Friedel–Crafts alkylation of aromatic halides or triflates promoted by protic or Lewis acids, it is generally assumed that the transformation occurs *via* the formation of a carbocation intermediate.⁷ The experimental results described above for this reaction, on the solid silica support under microwave irradiation suggest that: i) The reaction should not occur *via* a true carbocation intermediate because, in spite of the observation that basic additives inhibit the transformation, protic acids also do, however to a lesser extent and, if the carbocation is formed it is expected that for the substrates containing the propane **2b** or pentane **2c** alkyl chain and the intermolecular attempt (phenanthrene and 1,4-dibromobutane, Table 2, entry 5) some transformation of the starting bromide to other products should occur, which was not the case. ii) The true radical mechanism is also inconsistent, because low conversion was observed in the presence of (*n*-Bu₃Sn)₂ and, in spite of considerable observed inhibition in the presence of BHT, if the free radical intermediate was formed, it is expected that the substrate **2b**, containing the propane chain, should also react, because of the more favourable 5-*exo* cyclization. On the other hand, all results obtained are consistent with the occurrence of a more concerted reaction of C–Br breaking and C–Aryl bond formation, where the prior effective approach should be crucial, as depicted in Scheme 3. The effect of the



Scheme 3 Possible mechanism for the cyclization. The energy of the *ts* can be proportional to that of the carbocation.

additives could be rationalised from structural changes on the active surface silica reaction environment, which effects the stabilization of the reaction transition state.

The experimental results obtained clearly demonstrate that the Friedel–Crafts alkylation of bromoarylalkanes, supported in silica, under microwave irradiation, is extremely dependent on the substrate structure. These results, motivated us to perform a theoretical study of such systems, with the aim of understanding the reaction mechanisms. For that we used several of the experimental structures, together with others we needed for reasons which will be explained during the rest of this discussion (Fig. 1).

Table 4 Relative energies, by comparison with one of the table entries, of the carbocations formed as possible intermediaries in the cyclization of substrate **2** to product **3**

Entry	2	3	Conversion (%)	$\Delta G/\text{kJ mol}^{-1}$ relative to j	$\Delta G/\text{kJ mol}^{-1}$ rel. to a, g or j
1	a	a	94	-27.55	0.00 a
2	b	b	Sm	-12.24	15.31 a
3	c	c	Sm	-6.30	21.25 a
4	e	e	Complete	-21.23	6.32 a
5	d	d	Sm	-15.61	
6	f	f	94	3.26	20.85 g
7	f	f'	—	11.08	28.67 g
8	g	f	Complete	-17.59	0.00 g
9	g	g	—	11.90	29.49 g
10	n	n	—	7.36	24.95 g
11	h	h	76	1.52	
12	i	i	17	41.60	41.60 j
13	j	j	Complete	0.00	0.00 j
14	k	k	19	29.04	29.04 j
15	l	l	—	68.52	68.52 j
16	m	m	—	62.11	62.11 j

Sm = starting material.

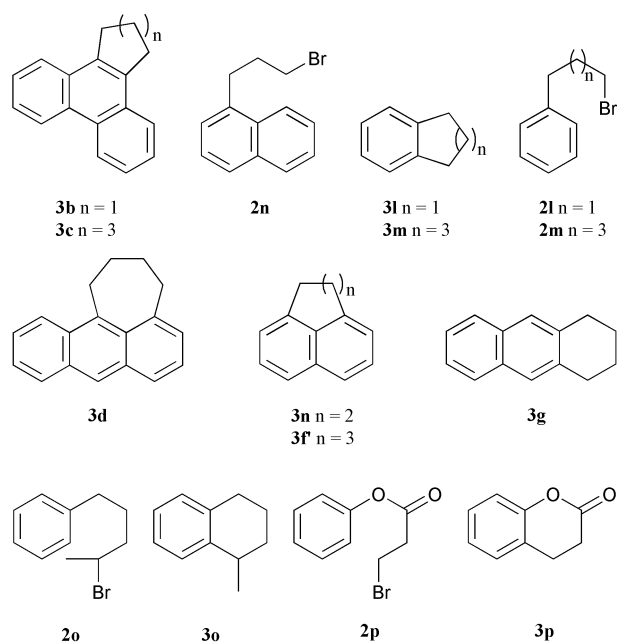


Fig. 1 Additional compound structures used in the theoretical study.

A priori, we could imagine three different mechanisms which, in turn, could be radical or ionic. The ionic ones could be S_N1 or S_N2 types. However, considering the experimental results, as mentioned before, the radical or the ionic S_N1 type mechanisms should not occur, since, with one exception (compound **4**), we didn't observe elimination products, even when the cyclisation does not occur. In these situations, only initial material was recovered. We have also to consider the medium where the reaction is taking place. In fact when considering reactions in solution, ionic mechanisms are in many cases possible due to the strong stabilization arising from the ion solvation. Even so, usually Friedel–Crafts alkylation or acylation reactions require the use of strong Lewis acids, in order to promote the ion pair formation. In our case, strong Lewis acids are not used and strong solvation should not be occurring. This means that the reaction should be an S_N2 type mechanism, where the attacking group approaches the aromatic ring, due to the high efficiency of microwaves, to be converted into internal molecular energy. The S_N2 type mechanism could be either an attack on the α carbon, as in Scheme 3, or an *ipso* attack, with the formation of a 5 membered ring *ts* or intermediary, which would migrate forming the final observed product. We dismissed this second possibility since, in those cases where no cyclization was

observed, one would expect elimination products, which were never observed.

Other experimental data which makes us prefer the ionic S_N2 type mechanism, is the observation that the addition of ionic substances, radical initiators or inhibitors does not seem to change the reaction behaviour.

Our first approach in studying the S_N2 type mechanisms, was a calculation of the transition state structures (*ts*). However *ts* structures are difficult to find and, usually, demand a large amount of computer time. Due to this we took another approach; in very similar structures, we can expect that the energy of the carbocation formed after the cyclization will be directly proportional to the energy of the respective transition state (Scheme 3), since there is no kind of interaction between the leaving bromide and the rest of the molecule. When we perform the calculations in the gas phase, no ion stabilization due to solvation is possible and, as a consequence, the energy of the carbocation and the separated bromide will be much higher than that of the transition state, where the charges partially cancel themselves. Even so, if the energy increase due to charge separation is similar in all structures, then the relative energies of the carbocations should be proportional to the relative energies of the transition states. The results[†] of our calculations are shown in Table 4.

The values from Table 4 seemed to fluctuate so in order to analyse them, we had to first make a few statements.

In spite of all the compounds being aromatic, we divided the structures into benzene, naphthalene, phenanthrene, anthracene or pyrene derivatives. Since the positive charge is dissipated in the full aromatic system, we can expect that for large systems the energy increase due to charge formation would be less than for small molecules. This becomes even more important if we think that there is no stabilization due to solvation.

Since we wanted to make a qualitative comparison between our theoretical results and the experimental observations (it is not possible to make a kinetic study in the experimental conditions we used, which means that we can only compare the calculated energies with the experimental conversions), we have to also consider that for some structures there are two equivalent reactive carbons while, for others, there is only one. Due to this statistical problem, after the same reaction time,

[†] All structure minimizations were calculated in the gas phase, using Gaussian 98,²² and *ab initio* HF theory with a 6-31G** basis set. The energies were calculated in the gas phase, as single points, using MP2 theory with a 6-31G** basis set and with thermal energy correction for 298.15 K and 1.00 atm.

Table 5 Transition state calculated energies ($\Delta G_{\ddagger}^{\ddagger} = \Delta G_{\text{ts}} - \Delta G_{\text{reag}} + \Delta G_{\text{Br}^-}$)

	2	3	Conv. (%)	$\Delta G_{\ddagger}^{\ddagger}/\text{kJ mol}^{-1}$	$\Delta G/\text{kJ mol}^{-1}$ rel. to j	$\Delta G/\text{kJ mol}^{-1}$ rel. to a, g or j
1	a	a	94	44.48	-10.87	0.00 a
2	b	b	Sm	92.53	37.18	48.05 a
3	c	c	Sm	68.77	13.42	24.29 a
4	e	e	Complete	—	—	—
5	d	d	Sm	73.35	18.00	—
6	f	f	94	62.72	7.37	11.98 g
7	f	f'	—	75.19	19.84	24.45 g
8	g	f	Complete	50.74	-4.61	0.00 g
9	g	g	—	73.39	18.04	22.65 g
10	n	n	—	84.55	29.20	33.81 g
11	h	h	76	70.85	15.50	—
12	i	i	17	71.06	15.71	15.71 j
13	j	j	Complete	55.35	0.00	0.00 j
14	k	k	19	65.94	10.59	10.59 j
15	l	l	—	119.00	63.65	63.65 j
16	m	m	—	99.00	43.65	43.65 j
17	p	p	— ^a	76.55	21.20	21.20 j
18	o	o	—	57.08	1.73	1.73 j

Sm = starting material. ^a In case of the analog substrate **4** was observed the formation of the olefin **5** as the only reaction product.

even for similar reactivities, the yield for both types of compounds can be considerably different.

Even after these considerations, if one tries to analyse the results in Table 4, using column 5, it is easy to conclude that a direct comparison between different families of compounds is not possible. In fact, we can see in entry 12 a conversion of 17%, for a relative energy of 41.6 kJ mol⁻¹, while the compound in entry 2 does not react, even considering that the relative energy of its carbocation is -12.2 kJ mol⁻¹. On the other hand, if we analyse the results by families of compounds, as depicted in column 6, it is possible to see a quite good agreement between theory and practice.

For benzene derivatives we can see that structure **2j** is expected to be the most reactive one, as in fact it is. Structures **2k** and **2i** show very similar experimental results, but the relative energies of their respective carbocations have a difference of about 11 kJ mol⁻¹. Nevertheless, since structure **2i** has two reactive carbons, the theoretical and experimental results can be considered in good agreement.

For the naphthalene derivatives, the experimental results are those in entries 6 to 8. Structure **2g** seems to be the most reactive one, in agreement with the theoretical results. In spite of its carbocation having near 21 kJ mol⁻¹ higher energy, structure **2f** is still very reactive. Structure **3f'** would be formed through an attack on the second aromatic ring. In practice this was not observed, which is in agreement with the theoretical results. However, the energy difference between the two possible carbocations of structure **2f** is only about 8 kJ mol⁻¹. Structure **3g** would be formed from structure **2g**, through an attack on position 3, instead of position 1. The difference in energy of near 30 kJ mol⁻¹ explains why only compound **3f** is formed.

For the phenanthrene derivatives, compound **2e** is the experimentally most reactive. The calculations say that it should be structure **2a**. In spite of this, the energy difference is small and the result is acceptable. Structures **2b** and **2c** seem to not react at all, in the experimental conditions we used. This result is in agreement with the calculations, since one intermediary has around 15 kJ mol⁻¹ higher energy than that of intermediary of **2a**, while the other has more than 21 kJ mol⁻¹ higher energy. Nevertheless it is interesting to compare the energies for intermediaries **2b** and **2c** with those of intermediaries of **2l** and **2m**, also with the formation of 5 and 7 membered rings respectively. Not only the large absolute difference but also the inversion of the relative energy differences (the formation of the seven membered ring is more favourable in the benzene derivative, while in the phenanthrene derivative it is the opposite), show that this approach can be useful but only when comparing very similar aromatic systems.

Given that the intermediary approach does not seem to perform very well, we decided to calculate the transition state energies of all the derivatives in Table 4.

As stated before, we already assumed that the transition state was of an ionic S_N2 type. Nevertheless, after accepting that, we discover another problem, which is the need for stabilization of the ionic species formed along the reaction path. In fact, one bromide and a proton are formed, at opposite sides of the molecule, which will increase the transition state energy to a value much higher than the real one, as it is exemplified in Fig. 2. Because of this, we decided to use small molecules or ions able to bind the transient ions in the transition state, lowering their energy. Considering the medium where the reactions are taking place, several possibilities were available, but the one which most simplifies the calculation process, is the use of bromide ion (Fig. 2). We believe that it is reasonable to use this ion, as the formation of this species occurs during the reaction. From a theoretical point of view, bromide is a bit heavy, as we are worked at the *ab initio* level. On the other hand, it does not increase the number of rotational or vibrational degrees of freedom, like polyatomic molecules or ions would do, and, on average, there was not a strong increase in the computational demand. The results of our calculations[‡] are shown in Table 5.

In contrast to the observations we made before for the calculation of carbocationic species, the values in columns 5 and 6 of Table 5, now seem much more consistent. When we compare

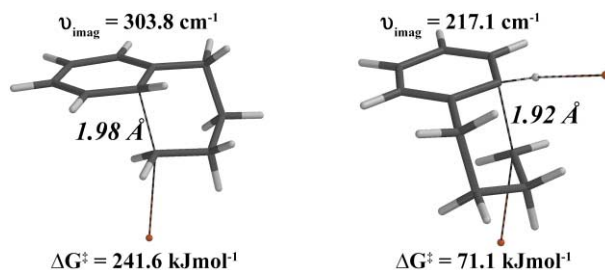


Fig. 2 Two possible *ts* structures for the cyclization. On the right side is depicted the model used for all the calculations, which uses a second bromide as a base for the proton removal.

[‡] All the transition states were minimized in the gas phase, using Gaussian 98,²² at *ab initio* HF theory with a 3-21G* basis set. The energies were calculated in the gas phase, as single points, at MP2 6-31G** and thermal energy was corrected for 298.15 K and 1.00 atm. The values were obtained after subtracting the energy of the transition state structures from the energy of the reagents plus the energy of a bromide ion.

entries 2 and 3 with entries 15 and 16 in Table 5, we can now see that in both cases the energy needed for the formation of the five membered ring is higher than that of the seven membered ring. In Table 4, one can see that this was not the case.

From entry 17, Table 5, it is possible to conclude that substrate **2p**, which is a model of compound **4**, is just on the border between the reactive and the non-reactive molecules. Since there is, in this compound, a second reaction path leading to elimination products through a low energy transition state, no cyclisation is observed for **4** but, instead, only the respective olefin **5** was observed.

Entry 18 in Table 5 corresponds to the transition state of a secondary bromide. In practice we tested this reaction with a phenanthrene derivative (entry 4, Table 5), but the transition state we obtained was of low quality. Even for the *ts* in entry 18 the structure was not the best, as indicated by the imaginary frequency, of only around 90 cm^{-1} , against more than 200 cm^{-1} for all the other transition states found. This happens because the potential energy surface is extremely flat for compound **2o** and, even more, for compound **2e**, making it very difficult to find good transition structures in these situations. After following a reaction path for structure **2o**, we believe that the energy shown in entry 18 should be increased to ~ 3 to 5 kJ mol^{-1} . Even so, we can conclude that the presence of the methyl group does not increase the steric hindrance but, on the other hand, stabilizes the positive charge formed during the reaction path (as soon as the C–Br bond length increases), lowering the transition state energy.

In spite of now being able to postulate the behaviour of these types of reaction, it is also very important to understand the differences or similarities in that behaviour. For compounds like those in entries 12, 15 and 16 (Table 5), it is easy to understand the relative behaviour, based on different ring strains. The five membered ring is the most energy demanding, while the six membered ring is the easiest one to be formed. But, when we compare for instance, the compounds in entries 12, 13, 14 or even 17 where all the transition states have six member rings, an electronic analysis[§] is necessary in order to understand the observed differences.

In principle the reaction should take place between the HOMO and the LUMO of the same molecule but, as we are dealing with large conjugated systems, it is possible, as we will see for some cases, that higher or lower energy orbitals have to be considered.

Starting with compound **2j** from entry 13, we can see that the HOMO orbital is located over carbons 2 and 6, the atoms which will suffer the attack (Fig. 3). In these carbons the HOMO coefficients are of around 0.25 and this structure has a high reactivity and a low transition state energy.



Fig. 3 HOMO orbitals ($0.032\text{ e}^{-}\text{ au}^{-3}$) for structures **2j** (left) and **2i** (right) (MP2/6-31G**//HF/6-31G**).

If we compare the HOMO of compound **2i**, entry 12, we can see that the orbital is located also over carbons 2 and 6, but the coefficients are much lower (0.15) (Fig. 3). Higher coefficients are found in carbons 1 (0.26) and 4. This structure still reacts in

the experimental conditions we used, but at a much slower rate, with around a 16 kJ mol^{-1} higher energy transition state, relative to structure **2j**.

The HOMO orbital of compound **2k** is shown in Fig. 4. It is possible to see there is no density over carbon 6, which means that the reacting orbital has to be a lower energy one. In this case it is the HOMO-1, which has a coefficient of 0.24 over carbon 6. In spite of being a high coefficient, this orbital is not as reactive as the HOMO would be for the same coefficient. Even so, considering the transition state energy of this compound (around 10.6 kJ mol^{-1} higher than the *ts* energy of structure **2j**), the low reactivity will be a result of its electronic configuration, of having only one reactive carbon and also, due to the presence of the large substituent, difficulty in the rotation of the side chain.

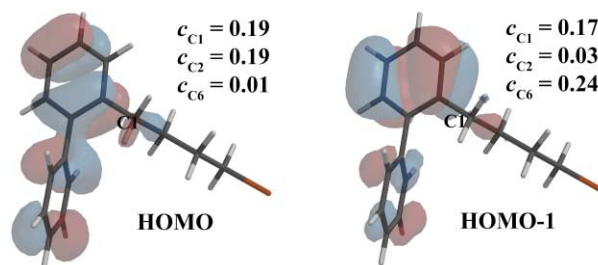


Fig. 4 HOMO (left) and HOMO-1 (right) orbitals ($0.032\text{ e}^{-}\text{ au}^{-3}$) for structure **2k** (MP2/6-31G**//HF/6-31G**).

Compound **2p** has a *ts* energy of around 21.2 kJ mol^{-1} , relative to compound **2j**, which is on the border of reacting/non-reacting. Its HOMO orbital has a shape similar to that of compound **2i**, with equal coefficients over carbons 2 and 6 (0.15). Nevertheless, the anti-ligand orbital which can react is, in this case, the LUMO + 2, since both the LUMO and LUMO + 1 have very low coefficients over the carbon connected to the bromine atom. Together with the higher ring strain due to the strong planarity of the transition state, these factors render a low reaction rate, associated with higher *ts* energy, when compared with compound **2i** (Fig. 5).

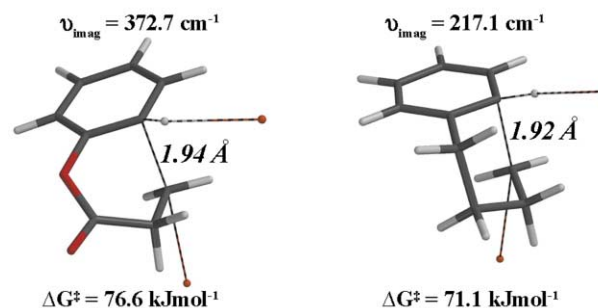


Fig. 5 Comparison of the transition state structures of compound **2p** (left) and **2i** (right).

Another family of compounds which has to be studied considering the electronic aspects, is the naphthalene derivatives. If we compare the transition state structures in Fig. 6, we can't see any important geometrical or steric differences explaining the reactivity. However, if we analyse the HOMO orbitals of the two possible derivatives (Fig. 7), we can easily understand the different behaviours.

For both isomers, the HOMO orbital has larger coefficients over carbons 1, 4, 5, and 8. When the substituent is in the ring position 1 (structure **2f**), the coefficient of carbon 1 is 0.21, of carbon 2 is 0.15, of carbon 3 is 0.15 and of carbon 8 is 0.20. When the substituent is in ring position 2 (structure **2g**), the coefficient of carbon 1 is 0.22, of carbon 2 is 0.17, of carbon 3 is 0.12 and of carbon 8 is 0.21. This large difference in the HOMO

[§] All structures were minimized in the gas phase, using Gaussian 98,²² at *ab initio* HF theory with a 6-31G** basis set. The surfaces were obtained from single point calculations, in the gas phase, at MP2 6-31G**, using Spartan '02 for Macintosh, v.1.0.3.²³

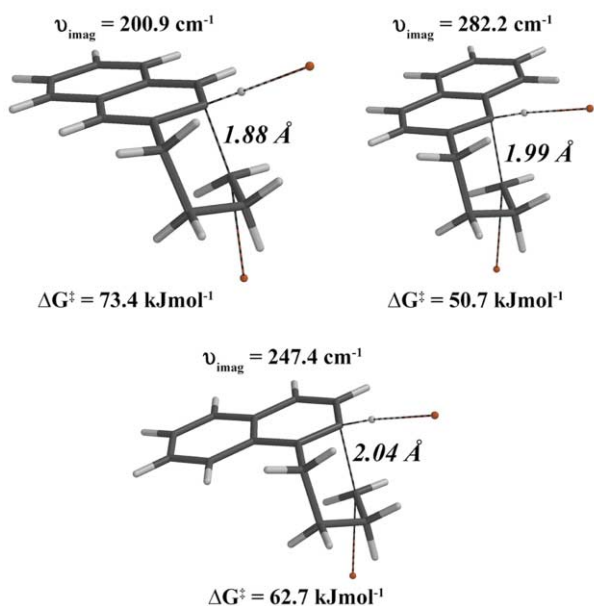


Fig. 6 Three *ts* structures for the cyclization reaction of naphthalene derivatives. **2g** to **3g** (top left); **2g** to **3f** (top right) and **2f** to **3f** (bottom).

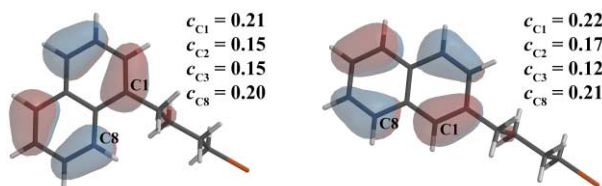


Fig. 7 HOMO orbitals ($0.032 e^- au^{-3}$) for structures **2f** (left) and **2g** (right) (MP2/6-31G**//HF/6-31G**).

distribution can explain the difference of nearly 23 kJ mol^{-1} between the two possible transition states of compound **2g**, indicating that it should react preferentially through carbon 1, as is experimentally observed. For isomer **2f**, we would expect, from the analysis of the HOMO distribution, that carbon 8 should be preferentially attacked. However, this is not what the transition state energy or the experimental results suggest. In this case, the main factor controlling the *ts* energy is the ring strain, due to the ring size and to the three coplanar carbon atoms (Fig. 8). The ring strain is even higher when a six membered ring is formed (structure **3n**, *ts* in Fig. 8). In this case, and also due to the three coplanar carbon atoms, the transition state adopts a boat conformation, while the transition states in Fig. 6 all have chair conformations.

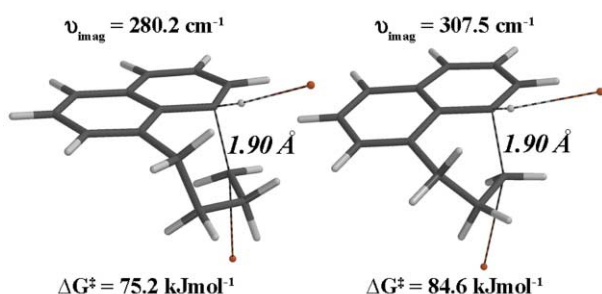


Fig. 8 *ts* Structures for the attack of carbon 8 in naphthalene derivatives. Formation of a seven membered ring (**3f'**, left) and formation of a six member ring (**3n**, right).

The phenanthrene and the anthracene derivatives are identical cases to those of benzene and naphthalene structures and do not need to be discussed in detail. The phenanthrene derivative **2a** has a HOMO orbital with a high density (0.21) over carbon 10, the reacting carbon. This value, similar to those

obtained for the benzene or naphthalene derivatives, does not explain the theoretically expected and experimentally observed higher reactivity. Also, since the phenanthrene and the naphthalene derivatives have only one reactive site for each isomer (all structures have more than one possible reactive carbon but not equivalents), opposite to some of the benzene derivatives, to get similar final yields they must have lower energy transition states. The *ts* energies agree with the experimental results, but they don't explain why. We believe that the differences between each family of compounds is due to considerable differences in the energy gap between the reactive ligand and the reactive anti-ligand orbitals (as we said before, they are not always the HOMO and the LUMO). Compound **2p** has an energy gap of 1294 kJ mol^{-1} . The average of the benzene derivatives (excluding compound **2p**) has an energy gap of 1210 kJ mol^{-1} . The average of the naphthalene derivatives has an energy gap of 1163 kJ mol^{-1} . Finally, the phenanthrene derivative has an energy gap of 1115 kJ mol^{-1} . These values are in good agreement with the experimental results and with the *ts* calculated values.

To finish this discussion we would like to point out a few more aspects concerning some special characteristics of the transition states, which can shed a bit more light over the total mechanism.

As we said in the beginning of our modelling discussion, we used a second bromide ion in order to simulate a solvent effect, reducing the transition state energy. Otherwise the charge separation would enormously increase the energy, as seen in Fig. 2 for the simplest benzene derivative. However, as the reactions were performed in the solid state, the diffusion of molecules or ions has to be slow, making it difficult for a bromide ion to reach a substrate molecule and act as a base. Of course, we can think about the solid matrix acting as a base, abstracting the proton and lowering the *ts* energy. But, if one looks at all the transition states we have calculated including those in Fig. 8 we notice that the electrophilic carbon has, in the transition state, a geometry away from planarity with valence angles of around 100 degrees. Also, the bromine-carbon bond has a length of about 3.1 \AA , while it should be around 2.5 \AA .⁸ These observations, together with the very flat transition state energy surfaces, as stated before, give the indication that, in the transition state, the bromine atom bond is almost ionic. This means that the bromine atom can rotate around the substrate (with some limitations), without changing the potential energy much. In this situation, we would suggest that the cyclisation can occur as a uni-molecular process, where the electrophilic carbon would approach the aromatic ring, followed by a rotation of the bromine to a position where it can abstract the hydrogen atom.

Conclusions

The study presented here clearly demonstrates that the intramolecular Friedel-Crafts alkylation of 4-aryl-1-bromobutanes immobilised on silica, under microwave irradiation, in dry media, is a simple, clean and efficient method for the synthesis of a range of fused polynuclear hydrocarbons. The range of substrate structures tested and the diverse experimental conditions used prompted us to perform a more complete modelling study of this transformation, which allowed a rationalisation of the observed peculiar dependence of the transformation on the substrate structure and, also, additional support for a concerted ionic mechanism.

The study presented here enables the anticipation that taking into consideration the effect of both *n*-alkyl bromide chains and aryl functionalities on this transformation, a large range of other fused polynuclear hydrocarbons can be synthesised by the simple methodology described here. Additionally from an environmental point of view, liberation of the harmful hydrogen bromide as a by-product is also minimised by being mainly absorbed on silica.

Experimental

General remarks

Diethyl ether was pre-dried over sodium wire and distilled from sodium/benzophenone under a nitrogen atmosphere. Dichloromethane was distilled over calcium hydride powder under a nitrogen atmosphere. Flash chromatography was carried out using silica MN-Kiesel-gel 60M gel (230–400 mesh ASTM, Art. 815381). All eluents were distilled prior to use. The NMR spectra were recorded on a Bruker AMX 400 in deuteriochloroform; chemical shifts (δ) were quoted in ppm against tetramethylsilane (TMS) and coupling constants in Hz. Infrared spectra (IR) were recorded on a Mattson FTIR Satellite 3000 spectrometer as thinly dispersed films (from dichloromethane). Melting points (uncorrected) were determined on a Electrothermal Mod. IA 6304 capillary melting point apparatus. Microanalyses were carried out at the *Laboratório de Análises do QCFB/FCT/UNL*. The microwave irradiated reactions (MWI) were carried out in a domestic household oven Balay 3WM-2121.

The starting bromides and the cyclisation products were identified by comparison of their physical and spectroscopic data with those of commercially available compounds or those known from the literature. The assignment of the signals in the NMR spectra of the compounds was based on their characteristic chemical shifts and the multiplicity of the signals and were confirmed by 2D NMR techniques (COSY, NOESY, HMQC). As there are two groups of similar signals, methylene groups and aromatic protons, NOESY cross peaks are of great importance to a correct assignment. The signals of the protons of the methylene group, connected with the bromine atom, in the starting bromides are in an area free of other signals which provides the possibility of determining the conversions using ^1H NMR spectra of the crude reaction mixtures.

ω -Arylbromoalkanes. General procedure⁶

To a stirred solution of arylbromide (10 mmol) in anhydrous diethyl ether (20 mL) under an argon atmosphere, *n*-butyllithium (1.5 eq., 1.6 M in hexane) was slowly added at 0 °C followed by the addition of α,ω -dibromoalkane (4.0 eq.) which was then refluxed for 2 hours. The reaction mixture was cooled to room temperature, partitioned between diethyl ether (40 mL) and water (30 mL). The aqueous phase was extracted with diethyl ether (2 \times 20 mL), the combined organic phase were dried over MgSO_4 , evaporated *in vacuo* and purified by flash chromatography on silica gel using hexane as a mobile phase.

1-Bromo-4-(9-phenanthrenyl)butane¹⁰ (2a). 63% Yield; mp 115–116 °C (lit. 114.5–116.5 °C); ^1H NMR: 1.977 (m, 2H, CH_2 -2), 2.015 (m, 2H, CH_2 -3), 3.154 (t, 2H, *J* 7.2, CH_2 -4), 3.482 (t, 2H, *J* 6.4, CH_2 -1), phenanthrenyl protons 7.587 (s, 1H, CH-10), 7.614 (overlapped signals, 2H, CH-2, CH-3), 7.662 (overlapped signals, 2H, CH-6, CH-7), 7.839 (d, 1H, *J* 7.5, CH-1), 8.107 (d, 2H, *J* 7.0, CH-8), 8.664 (d, 1H, *J* 8.4, CH-4), 8.752 (d, 1H, *J* 7.1, CH-5); important cross peaks in COSY: 1.977/3.482, 2.015/3.154, 7.614/7.839, 7.614/8.664, 7.662/8.752, 7.662/8.107, NOESY: 3.154/7.587, 3.154/8.107, 7.587/7.839, 8.664/8.752; ^{13}C NMR: 28.57 (CH_2 -3), 32.48 (CH_2 -4), 32.69 (CH_2 -2), 33.59 (CH_2 -1), phenanthrenyl CH-carbons 122.44 (CH-4), 123.27 (CH-5), 124.28 (CH-8), 126.04 (CH-10), 126.19 (CH-2, CH-3), 126.56 (CH-6), 126.63 (CH-7), 128.04 (CH-1).

1-Bromo-3-(9-phenanthrenyl)propane^{6a} (2b). 22% Yield; mp 56–57 °C (lit. 55–57 °C); ^1H NMR: 2.329 (m, 2H, CH_2 -2), 3.259 (t, 2H, *J* 7.2, CH_2 -3), 3.477 (t, 2H, *J* 6.4, CH_2 -1), phenanthrenyl protons 7.576 (overlapped signals, 2H, CH-2, CH-3), 7.594 (s, 1H, CH-10), 7.622 (overlapped signals, 2H, CH-6, CH-7), 7.811 (d, 1H, *J* 7.2, CH-1), 8.069 (d, 1H, *J* 6.9, CH-8), 8.627 (d, 1H, *J* 7.9, CH-4), 8.714 (d, 1H, *J* 6.9, CH-5); important cross peaks

in COSY: 2.329/3.259, 2.329/3.477, 7.567/7.811, 7.567/8.627, 7.622/8.069, 7.622/8.714, NOESY: 3.259/7.594, 3.259/8.069, 7.594/7.811, 8.627/8.714; ^{13}C NMR: 31.55 (CH_2 -3), 32.83 (CH_2 -2), 33.55 (CH_2 -1), phenanthrenyl CH-carbons 122.43 (CH-4), 123.30 (CH-5), 124.21 (CH-8), 126.17 (CH-7), 126.27 (CH-6), 126.68 (CH-2, CH-3, CH-10), 128.09 (CH-1).

1-Bromo-5-(9-phenanthrenyl)pentane¹⁰ (2c). 43% Yield; mp 74–75 °C (lit. 72–74.5 °C); ^1H NMR: 1.542 (m, 2H, CH_2 -3), 1.767 (m, 2H, CH_2 -4), 1.863 (m, 2H, CH_2 -2), 3.042 (t, 2H, *J* 7.4, CH_2 -5), 3.347 (t, 2H, *J* 6.7, CH_2 -1), phenanthrenyl protons 7.510 (s, 1H, CH-10), 7.541 (overlapped signals, 2H, CH-2, CH-3), 7.598 (overlapped signals, 2H, CH-6, CH-7), 7.778 (d, 1H, *J* 6.7, CH-1), 8.025 (d, 1H, *J* 7.8, CH-8), 8.596 (d, 1H, *J* 7.0, CH-4), 8.679 (d, 1H, *J* 6.8, CH-5); important cross peaks in COSY: 1.542/1.767, 1.542/1.863, 1.767/3.042, 1.863/3.347, 7.541/7.778, 7.541/8.596, 7.598/8.025, 7.598/8.679, NOESY: 3.042/7.510, 3.042/8.025, 7.510/7.778, 8.596/8.679; ^{13}C NMR: 28.34 (CH_2 -3), 29.31 (CH_2 -4), 32.72 (CH_2 -2), 33.22 (CH_2 -5), 33.80 (CH_2 -1), phenanthrenyl CH-carbons 122.31 (CH-4), 123.12 (CH-5), 124.19 (CH-8), 125.82 (CH-2), 125.90 (CH-3), 126.00 (CH-10), 126.37 (CH-7), 126.47 (CH-6), 127.89 (CH-1).

1-Bromo-4-(9-anthracenyl)butane^{6c} (2d). 42% Yield; mp 114.5–116 °C (lit. 115–116 °C); ^1H NMR: 1.995 (m, 2H, CH_2 -3), 2.136 (m, 2H, CH_2 -2), 3.503 (t, 2H, *J* 6.8, CH_2 -4), 3.664 (t, 2H, *J* 8.0, CH_2 -1), anthracenyl protons 7.491 (overlapped signals, 2H, CH-3, CH-6), 7.549 (overlapped signals, 2H, CH-2, CH-7), 8.030 (d, 2H, *J* 8.0, CH-4, CH-5), 8.273 (d, 2H, *J* 8.8, CH-1, CH-8), 8.365 (s, 1H, CH-10); important cross peaks in COSY: 1.995/3.503, 2.136/3.664, 7.491/8.030, 7.549/8.273, NOESY: 3.503/8.273, 8.030/8.365; ^{13}C NMR: 26.90 (CH_2 -3), 29.60 (CH_2 -4), 32.98 (CH_2 -2), 33.46 (CH_2 -1), anthracenyl CH-carbons 124.17 (CH-1, CH-8), 124.79 (CH-3, CH-6), 125.55 (CH-2, CH-7), 125.84 (CH-10), 129.23 (CH-4, CH-5).

2-Bromo-5-(9-phenanthrenyl)pentane (2e). 47% Yield; mp 76–77 °C; IR: 705, 738, 896, 1265, 1422, 2305, 2945, 2987, 3054 cm^{-1} ; ^1H NMR: 1.722 (d, 3H, *J* 6.6, CH_3), 1.981 (m, 2H, CH_2 -3), 2.058 (m, 2H, CH_2 -4), 3.148 (m, 2H, CH_2 -5), 4.211 (m, 1H, CH-2), phenanthrenyl protons 7.581 (s, 1H, CH-10), 7.591 (overlapped signals, 2H, CH-2, CH-3), 7.656 (overlapped signals, 2H, CH-6, CH-7), 7.838 (d, 2H, *J* 7.1, CH-1), 8.093 (d, 1H, *J* 6.8, CH-8), 8.658 (d, 1H, *J* 8.0, CH-4), 8.738 (d, 1H, *J* 6.6, CH-5); important cross peaks in COSY: 1.722/4.211, 1.981/4.211, 2.058/3.148, 7.591/7.838, 7.591/8.658, 7.656/8.093, 7.656/8.738, NOESY: 3.148/7.581, 3.148/8.093, 7.581/7.838, 8.658/8.738; ^{13}C NMR: 26.48 (CH_3), 28.23 (CH_2 -4), 32.65 (CH_2 -5), 40.99 (CH_2 -3), 51.46 (CH-2), phenanthrenyl CH-carbons 122.42 (CH-4), 123.24 (CH-5), 124.29 (CH-8), 126.00 (CH-10), 126.14 (CH-2, CH-3), 126.58 (CH-6), 126.60 (CH-7), 128.03 (CH-1); Anal. calc. for $\text{C}_{19}\text{H}_{19}\text{Br}$: C 69.73, H 5.85; Found C 69.91, H 5.81%.

1-Bromo-4-(1-naphthyl)butane⁹ (2f). 39% Yield; colourless oil; ^1H NMR: 1.844 (m, 2H, CH_2 -3), 1.899 (m, 2H, CH_2 -2), 3.032 (t, 2H, *J* 6.9, CH_2 -4), 3.369 (t, 2H, *J* 6.5, CH_2 -1), naphthyl protons 7.262 (d, 1H, *J* 6.9, CH-2), 7.357 (dd, 1H, *J* 7.0, 8.4, CH-3), 7.434 (dd, 1H, *J* 6.8, 8.5, CH-6), 7.479 (dd, 1H, *J* 6.9, 8.4, CH-7), 7.681 (d, 1H, *J* 8.5, CH-4), 7.816 (d, 1H, *J* 8.5, CH-5), 7.987 (d, 1H, *J* 8.5, CH-8); important cross peaks in COSY: 1.899/3.369, 1.844/3.032, 7.262/7.357, 7.357/7.681, 7.434/7.816, 7.479/7.987, NOESY: 3.032/7.262, 3.032/7.987, 7.681/7.816; ^{13}C NMR: 29.21 (CH_2 -3), 32.14 (CH_2 -4), 32.71 (CH_2 -2), 33.64 (CH_2 -1), naphthyl CH-carbons 123.73 (CH-8), 125.54 (CH-3, CH-6), 125.87 (CH-7), 126.02 (CH-2), 126.79 (CH-4), 128.86 (CH-5).

1-Bromo-4-(2-naphthyl)butane¹¹ (2g). 44% Yield; colourless oil; ^1H NMR: 1.876 (m, 2H, CH_2 -3), 1.916 (m, 2H, CH_2 -2), 2.798 (t, 2H, *J* 7.2, CH_2 -4), 3.423 (t, 2H, *J* 6.4, CH_2 -1), naphthyl

protons 7.321 (d, 1H, *J* 8.5, CH-3), 7.416 (dd, 1H, *J* 7.2, 8.1, CH-6), 7.453 (dd, 1H, *J* 7.3, 8.4, CH-7), 7.605 (s, 1H, CH-1), 7.772 (d, 2H, *J* 8.1, CH-4, CH-8), 7.805 (d, 1H, *J* 7.7, CH-5); important cross peaks in COSY: 1.876/2.798, 1.916/3.423, 7.321/7.772, 7.416/7.805, 7.453/7.772, NOESY: 2.798/7.605, 2.798/7.321, 1.876/7.321, 7.605/7.772; ¹³C NMR: 29.65 (CH₂-3), 32.20 (CH₂-2), 33.64 (CH₂-1), 35.08 (CH₂-4), naphthyl CH-carbons 125.18 (CH-6), 125.94 (CH-7), 126.40 (CH-1), 127.16 (CH-3), 127.39 (CH-8), 127.59 (CH-4), 127.95 (CH-5).

1-Bromo-4-(1-pyrenyl)butane¹² (**2h**). 28% Yield; mp 71–72 °C; ¹H NMR: 2.026 (m, 4H, CH₂-2, CH₂-3), 3.372 (t, 2H, *J* 7.0, CH₂-4), 3.467 (t, 2H, *J* 6.2, CH₂-1), pyrenyl protons 7.859 (d, 1H, *J* 7.8, CH-2), 7.996 (dd, 1H, *J* 7.6, CH-7), 8.031 (overlapped signals, 2H, CH-4, CH-5), 8.115 (overlapped signals, 2H, CH-3, CH-9), 8.168 (d, 1H, *J* 7.4, CH-6), 8.174 (d, 1H, *J* 7.4, CH-8), 8.268 (d, 1H, *J* 9.2, CH-10); important cross peaks in COSY: 2.026/3.372, 2.026/3.467, 7.859/8.115, 7.996/8.168, 7.996/8.174, 8.115/8.268, NOESY: 3.372/7.859, 3.372/8.268, 8.031/8.115, 8.031/8.168, 8.115/8.174; ¹³C NMR: 30.16 (CH₂-3), 32.55 (CH₂-2, CH₂-4), 33.52 (CH₂-1), pyrenyl CH-carbons 123.18 (CH-10), 124.73 (CH-6), 124.76 (CH-8), 124.88 (CH-3), 125.80 (CH-9), 126.64 (CH-7), 127.15 (CH-2), 127.31 (CH-4), 127.44 (CH-5).

1-Bromo-4-phenylbutane¹³ (**2i**). 42% Yield; colourless oil; ¹H NMR: 1.782 (m, 2H, CH₂-3), 1.892 (m, 2H, CH₂-2), 2.642 (t, 2H, *J* 7.6, CH₂-4), 3.417 (t, 2H, *J* 6.7, CH₂-1), 7.178 (1H, *p*-Ph), 7.197 (2H, *o*-Ph), 7.285 (2H, *m*-Ph); important cross peaks in COSY: 1.892/3.417, 1.782/2.642, NOESY: 2.642/7.197; ¹³C NMR: 29.844 (CH₂-3), 32.247 (CH₂-2), 33.643 (CH₂-1), 34.974 (CH₂-4), 125.91 (*o*-Ph), 128.38 (*m*-Ph, *p*-Ph).

1-Bromo-4-(3,5-dimethylphenyl)butane¹⁴ (**2j**). 56% Yield; colourless oil; ¹H NMR: 1.735 (m, 2H, CH₂-3), 1.881 (m, 2H, CH₂-2), 2.555 (t, 2H, *J* 7.6, CH₂-4), 3.434 (t, 2H, *J* 6.8, CH₂-1), 2.283 (s, 6H, CH₃), 6.790 (2H, *o*-Ph), 6.824 (1H, *p*-Ph); important cross peaks in COSY: 1.735/2.555, 1.881/3.434, NOESY: 2.555/6.790; ¹³C NMR: 21.33 (CH₃), 29.96 (CH₂-3), 32.41 (CH₂-2), 33.70 (CH₂-1), 34.88 (CH₂-4), 126.27 (*o*-Ph), 127.57 (*p*-Ph).

1-Bromo-4-(2-biphenyl)butane¹⁵ (**2k**). 22% Yield; colourless oil; ¹H NMR: 1.581 (m, 2H, CH₂-3), 1.705 (m, 2H, CH₂-2), 2.592 (t, 2H, *J* 7.7, CH₂-4), 3.216 (t, 2H, *J* 6.8, CH₂-1), biphenyl protons 7.296 (d, 1H, *J* 7.8, CH-3), 7.317 (overlapped signal, 1H, CH-9), 7.330 (overlapped signal, 1H, CH-4), 7.364 (overlapped signal, 1H, CH-5), 7.387 (d, 2H, *J* 7.7, CH-7, CH-11), 7.426 (d, 1H, *J* 6.5, CH-6), 7.483 (dd, 2H, CH-8, CH-10); important cross peaks in COSY: 1.581/2.592, 1.705/3.216, 7.296/7.330, 7.364/7.426, 7.317/7.483, 7.387/7.483, NOESY: 2.592/7.296, 2.592/7.387, 7.387/7.426; ¹³C NMR: 29.69 (CH₂-3), 32.03 (CH₂-4), 32.38 (CH₂-2), 33.50 (CH₂-1), biphenyl CH-carbons 125.91 (CH-3), 126.90 (CH-6), 127.49 (CH-4), 128.15 (CH-8, CH-10), 129.23 (CH-5, CH-7, CH-11), 130.14 (CH-9).

(9-Phenanthrenyl)-3-bromopropionate (**4**). To a stirred solution of 9-phenanthrol (194 mg, 1.0 mmol) and pyridine (0.4 mL, 5.0 mmol) in anhydrous dichloromethane (3 mL) at room temperature and under an argon atmosphere, 3-bromopropionyl chloride (0.2 mL, 1.75 mmol) was added. After 2 hours the reaction mixture was partitioned between dichloromethane (20 mL) and hydrochloric acid (10 mL). The organic phase was washed with brine, dried over MgSO₄, evaporated *in vacuo* and purified by flash chromatography on silica gel using 10% ethyl acetate in hexane as a mobile phase to give (**4**) (30 mg, 9%); mp 102–103 °C; IR: 705, 896, 1135, 1265, 1422, 1765, 2305, 2987, 3054, 3418 cm⁻¹; ¹H NMR: 3.272 (t, 2H, CH₂-1), 3.998 (t, 2H, CH₂-2), phenanthrenyl protons 7.563 (s, 1H, CH-10), 7.631 (overlapped signals, 2H, CH-2, CH-3), 7.714 (overlapped signals, 2H, CH-6, CH-7), 7.864 (d, 1H, *J* 7.6,

CH-1), 7.990 (d, 2H, *J* 8.0, CH-8), 8.675 (d, 1H, *J* 8.1, CH-4), 8.726 (d, 1H, *J* 8.3, CH-5); important cross peaks in COSY: 3.272/3.998, 7.631/7.864, 7.631/8.675, 7.714/7.990, 7.714/8.726, NOESY: 7.563/7.864, 8.675/8.726; ¹³C NMR: 37.78 (CH₂-1), 38.92 (CH₂-2), 149.45 (C=O), phenanthrenyl CH-carbons 117.69 (CH-10), 121.78 (CH-8), 122.63 (CH-4), 122.98 (CH-5), 126.56 (CH-2), 126.96 (CH-3), 127.06 (CH-7), 127.28 (CH-6), 128.48 (CH-1); FAB+ [M] 329 (3.54), [M – CO₂] 285 (18.52), [M – Br] 249 (23.04), [M – CH=CHBr] 223 (38.64), [McLaferty rearrangement] 194 (100.00).

General procedure for the microwave irradiation (MWI) reactions

To a solution of arylbromoalkane (1.0 mmol) in dichloromethane (5 mL) silica gel (2.0 g) was added and the solvent was removed *in vacuo*. The powder mixture was heated in a MW oven at 800 W for 15 min. After extraction from silica gel with dichloromethane, the conversions were determined by ¹H NMR spectroscopy of the crude reaction mixtures. The products were purified by flash chromatography on silica gel using hexane as a mobile phase.

1,2,3,4-Tetrahydrotriphenylene¹⁶ (**3a**). Starting bromide; 1-bromo-4-(9-phenanthrenyl)butane (**2a**); 95% conversion; isolated yield 91%; mp 119–120 °C (lit. 120–121 °C); ¹H NMR: 2.000 (m, 4H, CH₂-2, CH₂-3), 3.164 (t, 4H, *J* 6.4, CH₂-1, CH₂-4), 7.604 (overlapped signals, 4H, CH-6, CH-7, CH-10, CH-11), 8.065 (d, 2H, *J* 7.4, CH-5, CH-12), 8.695 (d, 2H, *J* 7.4, CH-8, CH-9); important cross peaks in COSY: 2.000/3.164, 7.604/8.065, 7.604/8.695, NOESY: 3.164/8.065; ¹³C NMR: 22.91 (CH₂-2, CH₂-3), 26.85 (CH₂-1, CH₂-4), 122.70 (CH-8, CH-9), 123.29 (CH-5, CH-12), 125.48 (CH-6, CH-11), 126.52 (CH-7, CH-10).

1-Methyl-1,2,3,4-tetrahydrotriphenylene (**3e**). Starting bromide; 1-bromo-1-methyl-4-(9-phenanthrenyl)butane (**2e**); 100% conversion; isolated yield 97%; mp 94–95 °C; IR 705, 739, 896, 1265, 1429, 1495, 2304, 2872, 2935, 2968, 3053, 3079 cm⁻¹; ¹H NMR: 1.436 (d, 3H, *J* 6.8, CH₃), 1.962 (m, 2H, CH₂-2), 2.096 (m, 2H, CH₂-3), 3.056 (m, 1H, CH₂-4), 3.307 (dd, 1H, *J* 5.6, 17.2, CH₂-4), 3.720 (m, 1H, CH-1), 7.614 (overlapped signals, 4H, CH-6, CH-7, CH-10, CH-11), 8.081 (d, 1H, *J* 6.0, CH-5), 8.149 (d, 1H, *J* 7.6, CH-12), 8.702 (overlapped signals, 2H, CH-8, CH-9); important cross peaks in COSY: 1.436/3.720, 1.962/3.720, 2.096/3.056, 2.096/3.307, 7.614/8.081, 7.614/8.702, 7.614/8.149, NOESY: 1.436/8.149, 3.720/8.149, 3.056/8.081, 3.307/8.081; ¹³C NMR: 17.549 (CH₃), 21.474 (CH₃), 26.501 (CH₂-4), 28.480 (CH-1), 29.752 (CH₂-2), 122.63 (CH-9), 122.88 (CH-8), 123.48 (CH-5), 123.92 (CH-12), 125.25 (CH-10), 125.52 (CH-11), 126.40 (CH-7), 126.50 (CH-6); Anal. calc. for C₁₉H₁₈ C 92.63, H 7.37; Found C 92.52, H 7.28%.

1,2,3,4-Tetrahydrophenanthrene¹⁷ (**3f**). a) Starting bromide; 1-bromo-4-(1-naphthyl)butane (**2f**); 94% conversion; isolated yield 91%; mp 31–32 °C (lit. 32–33 °C); ¹H NMR: 1.860 (m, 2H, CH₂-2), 1.970 (m, 2H, CH₂-3), 2.899 (t, 2H, *J* 5.8, CH₂-1), 3.101 (t, 2H, *J* 6.2, CH₂-4), 7.189 (d, 1H, *J* 8.5, CH-10), 7.412 (dd, 1H, *J* 8.2, 8.6, CH-7), 7.481 (dd, 1H, *J* 8.4, 8.5, CH-6), 7.598 (d, 1H, *J* 8.5, CH-9), 7.778 (d, 1H, *J* 8.5, CH-8), 7.955 (d, 1H, *J* 8.5, CH-5); important cross peaks in COSY: 1.860/2.899, 1.970/3.101, 7.189/7.598, 7.412/7.778, 7.481/7.955, NOESY: 2.899/7.189, 3.101/7.955, 7.598/7.778; ¹³C NMR: 22.96 (CH₂-2), 23.24 (CH₂-3), 25.67 (CH₂-1), 30.45 (CH₂-4), 122.82 (CH-5), 124.53 (CH-7), 124.80 (CH-9), 125.72 (CH-6), 128.24 (CH-10), 128.44 (CH-8). b) Starting bromide; 1-bromo-4-(2-naphthyl)butane (**2g**); 100% conversion; isolated yield 96%; identical mp and NMR data to the product described in a).

7,8,9,10-Tetrahydrobenzo[*a*]pyrene¹⁸ (**3h**). Starting bromide; 1-bromo-4-(1-pyrenyl)butane (**2h**); 76% conversion; isolated

yield 72%; mp 112–113 °C (lit. 113 °C); ¹H NMR: 1.986 (m, 2H, CH₂-8), 2.092 (m, 2H, CH₂-9), 3.232 (t, 2H, *J* 6.1, CH₂-7), 3.439 (t, 2H, *J* 6.3, CH₂-10), 7.895 (s, 1H, CH-6), 7.937 (overlapped signal, 1H, CH-4), 7.943 (overlapped signal, 1H, CH-2), 7.956 (overlapped signal, 1H, CH-1), 8.085 (d, 1H, *J* 9.6, CH-12), 8.108 (d, 1H, *J* 8.7, CH-5), 8.138 (d, 1H, *J* 7.6, CH-3), 8.233 (d, 1H, *J* 9.2, CH-11); important cross peaks in COSY: 1.986/3.232, 2.092/3.439, 7.937/8.108, 7.943/7.956, 7.943/8.138, 8.085/8.233, NOESY: 3.232/7.895, 3.439/8.233, 7.895/8.108, 7.937/8.138, 7.956/8.085; ¹³C NMR: 23.05 (CH₂-8), 23.51 (CH₂-9), 26.40 (CH₂-10), 30.89 (CH₂-7), 122.74 (CH-11), 124.63 (CH-3, CH-5), 125.28 (CH-2), 125.83 (CH-6), 126.43 (CH-4), 127.01 (CH-1), 127.16 (CH-12).

1,2,3,4-Tetrahydronaphthalene¹⁹ (Tetralin) (3i). Starting bromide; 1-bromo-4-phenylbutane (2i); 17% conversion; 13% isolated yield; colourless oil; ¹H NMR: 1.787 (m, 4H, CH₂-2, CH₂-3), 2.753 (t, 4H, *J* 6.5, CH₂-1, CH₂-4), 7.056 (m, 4H, CH-5, CH-6, CH-7, CH-8); important cross peak in COSY: 1.787/2.753, NOESY: 2.753/7.056; ¹³C NMR: 23.27 (CH₂-2, CH₂-3), 29.43 (CH₂-1, CH₂-4), 125.43 (CH-6, CH-7), 129.16 (CH-5, CH-8).

5,7-Dimethyl-1,2,3,4-tetrahydronaphthalene²⁰ (3j). Starting bromide; 1-bromo-4-(3,5-dimethylphenyl)butane (2j); 100% conversion; isolated yield 96%; colourless oil; ¹H NMR: 1.747 (m, 2H, CH₂-2), 1.811 (m, 2H, CH₂-3), 2.576 (t, 2H, *J* 6.5, CH₂-4), 2.726 (t, 2H, *J* 6.2, CH₂-1), 2.171 (s, 3H, CH₃-5), 2.245 (s, 3H, CH₃-7), 6.756 (s, 1H, CH-8), 6.801 (s, 1H, CH-6); important cross peak in COSY: 1.747/2.726, 1.811/2.575; NOESY: 2.726/6.756, 2.576/2.171, 2.171/6.801, 2.245/6.756; ¹³C NMR: 19.37 (CH₃-5), 20.79 (CH₃-7), 23.01 (CH₂-2), 23.57 (CH₂-3), 26.36 (CH₂-4), 30.06 (CH₂-1), 127.43 (CH-8), 127.96 (CH-6).

5-Phenyl-1,2,3,4-tetrahydronaphthalene²¹ (3k). Starting bromide; 1-bromo-4-(2-biphenyl)butane (2k); 19% conversion; 14% isolated yield; colourless oil; ¹H NMR: 1.629 (m, 2H, CH₂-3), 1.724 (m, 2H, CH₂-2), 2.512 (t, 2H, *J* 5.6, CH₂-4), 2.785 (t, 2H, *J* 6.5, CH₂-1), 6.961 (d, 1H, *J* 6.8, CH-6), 7.024 (d, 1H, *J* 6.8, CH-8), 7.086 (dd, 1H, CH-7), 7.213 (overlapped signal, 2H, *o*-Ph), 7.251 (overlapped signal, 1H, *o*-Ph), 7.321 (overlapped signal, 2H, *m*-Ph); important cross peaks in COSY: 1.629/2.512, 1.724/2.785, 6.961/7.086, 7.024/7.086, NOESY: 2.512/7.251, 2.785/7.024, 6.961/7.251; ¹³C NMR: 22.88 (CH₂-2), 23.32 (CH₂-3), 28.12 (CH₂-4), 29.90 (CH₂-1), 125.13 (CH-7), 126.60 (*p*-Ph), 127.03 (CH-6), 127.91 (*m*-Ph), 128.36 (CH-8), 129.15 (*o*-Ph).

(9-Phenanthrenyl)acrylate (5). Starting bromide; (9-phenanthrenyl)-3-bromopropionate (4); 66% conversion; 63% isolated yield; mp 69–70 °C; IR 705, 737, 896, 1153, 1265, 1422, 1745, 2305, 2987, 3054, 3438 cm⁻¹; ¹H NMR: 6.122 (dd, 1H, *J*²_{cis,trans} 1.2, *J*³_{H,Htrans} 10.5, H_{cis} of CH₂=), 6.514 (dd, 1H, *J*³_{H,Htrans} 10.5, *J*³_{H,Hcis} 17.3, CH=), 6.761 (dd, 1H, *J*²_{cis,trans} 1.2, *J*³_{H,Hcis} 17.3, H_{trans} of CH₂=), phenanthrenyl protons 7.588 (s, 1H, CH-10), 7.611 (overlapped signals, 2H, CH-2, CH-3), 7.689 (overlapped signals, 2H, CH-6, CH-7), 7.848 (d, 1H, *J* 7.7, CH-1), 7.954 (d, 2H, *J* 8.1, CH-8), 8.655 (d, 1H, *J* 8.0, CH-4), 8.706 (d, 1H, *J* 8.2, CH-5); important cross peaks in COSY: 6.514/6.122, 6.514/6.761, 7.611/7.848, 7.611/8.655, 7.689/7.954, 7.689/8.706, NOESY: 6.122/6.514, 6.122/6.761, 7.588/7.848, 8.655/8.706; ¹³C NMR: 127.74 (CH=), 133.04 (CH₂=), 164.56 (C=O), phenanthrenyl CH-carbons 117.70 (CH-10), 121.84 (CH-8), 122.64 (CH-4), 122.98 (CH-5), 126.46 (CH-3), 126.90 (CH-2), 127.04 (CH-7), 127.22 (CH-6), 128.49 (CH-1); Anal. Calc. for C₁₇H₁₂O₂ C 82.24, H 4.87; Found C 82.10, H 4.90%.

Acknowledgements

We thank Fundação para a Ciência e Tecnologia, FEDER (Ref. POCTI/QUI/42983/2001 and Ref. SFRH/BPD/5531/2001) and INVOTAN (Ref. OUTREACH) for financial support.

Notes and references

- Reviews: (a) S. Caddick, *Tetrahedron*, 1995, **51**, 10403; (b) S. Deshayes, M. Liagre, A. Loupy, J.-L. Luche and A. Petit, *Tetrahedron*, 1999, **55**, 10851; (c) P. Lidstrom, J. Tierney, B. Wathey and J. Westman, *Tetrahedron*, 2001, **57**, 9225; (d) A. Kirschning, H. Monenschein and R. Wittenberg, *Angew. Chem., Int. Ed.*, 2001, **40**, 650; (e) M. Larhed, C. Moberg and A. Hallberg, *Acc. Chem. Res.*, 2002, **35**, 717 and references cited therein.
- Reviews: (a) A. Loupy, A. Petit, J. Hamelin, F. Texier-Boullet, P. Jacquault and D. Mathe, *Synthesis*, 1998, 1213; (b) R. S. Varma, *Green Chemistry*, 1999, 43 and references cited therein.
- (a) E. Clar, *Polycyclic Hydrocarbons*, Academic Press, New York, 1964, vol. I, II; (b) F. Oesch, G. Stillger, H. Frank and K. L. Platt, *J. Org. Chem.*, 1982, **47**, 568; (c) A. T. Balaban, M. D. Gheorghiu, A. Schiketanz and A. Necula, *J. Am. Chem. Soc.*, 1989, **111**, 734; (d) R. M. Roberts, A. A. Khalaf, *Friedel-Crafts Alkylation Chemistry: A Century of Discovery*, Dekker, New York, 1984; (e) G. A. Olah, R. Krishnamurti, G. K. S. Prakash, *Friedel-Crafts Alkylations, in Comprehensive Organic Synthesis*, ed. B. M. Trost, Pergamon Press, Oxford, 1991, vol. 3, p. 293; (f) B. M. Trost and M. R. Ghandiri, *J. Am. Chem. Soc.*, 1984, **106**, 7260; (g) S. T. Bright, J. M. Coxon and P. J. Steel, *J. Org. Chem.*, 1990, **55**, 1338; (h) S. R. Angle and M. S. Louie, *J. Org. Chem.*, 1991, **56**, 2853; (i) I. Hachiro, M. Moriwaki and S. Kobayashi, *Bull. Chem. Soc. Jpn.*, 1995, **68**, 2053.
- (a) V. K. Bhalerao, B. S. Nanjundiah, H. R. Sonawane and P. M. Nair, *Tetrahedron*, 1986, **42**, 1487; (b) K. V. Subbarao, N. P. Damodaran and S. Dev, *Tetrahedron*, 1987, **43**, 2543; (c) P. J. Kropp and R. L. Adkins, *J. Am. Chem. Soc.*, 1991, **113**, 2709.
- A. Loupy, P. Pigeon and M. Ramdani, *Tetrahedron*, 1996, **52**, 6705.
- (a) A. Sugimoto, K. Sumi, K. Urakawa, M. Ikemura, S. Sakamoto, Sh. Yoneda and Y. Otsuji, *Bull. Chem. Soc. Jpn.*, 1983, **56**, 3118; (b) H. Cao, Y. Fujiwara, T. Haino, Y. Fukazawa, C.-H. Tung and Y. Tanimoto, *Bull. Chem. Soc. Jpn.*, 1996, **69**, 2801; (c) C. A. M. Afonso and J. P. S. Farinha, *J. Chem. Res.*, 2003, 584.
- J. March, *Advanced Organic Chemistry: Reactions, Mechanisms, and Structures*, John Wiley & Sons, New York, 1992.
- A. G. Santos, S. X. Candeias, C. A. M. Afonso, K. Jenkins, S. Caddick, N. R. Treweek and D. Pardoe, *Tetrahedron*, 2001, **57**, 6607.
- R. H. F. Manske and A. E. Ledingham, *Can. J. Res.*, 1939, **17B**, 14 (*Chem. Abstr.*, 1939, **33**, 53875).
- A. Sugimoto, R. Hiraoka, N. Fukada, H. Kosaka and H. Inoue, *J. Chem. Soc., Perkin Trans. 1*, 1992, 2871.
- (a) R. Huisgon and U. Rietz, *Chem. Ber.*, 1957, **90**, 2768; (b) P. Studt, *Ann. Chem.*, 1965, **685**, 49.
- K. Furuta, K. Tomokiyo, M. T. Kuo, T. Ishikawa and M. Suzuki, *Tetrahedron*, 1999, **55**, 7529.
- (a) L. Cherkasov, Kh. Balyan and V. Kormer, *Zh. Org. Khim.*, 1966, **2**, 1934; (b) K. Subbarao, N. Damodaran and S. Dev, *Tetrahedron*, 1987, **43**, 2543.
- R. Abramovitch and A. Kress, *J. Org. Chem.*, 1984, **49**, 3114.
- A. Gribble, R. Dolle, A. Shaw, D. McNair, R. Novelli, Chr. Novelli, Br. Slingsby, V. Shah, D. Tew, B. Saxty, M. Allen, P. Groot, N. Pearce and J. Yates, *J. Med. Chem.*, 1996, **39**, 3569.
- (a) E. Bergmann and O. Blum-Bergmann, *J. Am. Chem. Soc.*, 1937, **59**, 1441; (b) Z. Marcinow, A. Sygula and P. W. Rabideau, *J. Org. Chem.*, 1988, **53**, 3603.
- W. Bachmann and W. Struve, *J. Org. Chem.*, 1939, **4**, 472.
- (a) L. F. Fieser and M. Fieser, *J. Am. Chem. Soc.*, 1935, **57**, 782; (b) P. Fu, H. Lee and R. Harvey, *J. Org. Chem.*, 1980, **45**, 2797.
- Aldrich catalog, No. 52,265–1.
- E. de B. Barnett and F. G. Sanders, *J. Chem. Soc.*, 1933, 434.
- Y. Nakatsujii, T. Kubo, M. Nomura and Sh. Kikkawa, *Bull. Chem. Soc. Jpn.*, 1978, **51**, 618.
- M. J. Frisch, G. W. Trucks, H. B. Schlegel, G. E. Scuseria, M. A. Robb, J. R. Cheeseman, V. G. Zakrzewski, J. A. Montgomery, Jr., R. E. Stratmann, J. C. Burant, S. Dapprich, J. M. Millam, A. D. Daniels, K. N. Kudin, M. C. Strain, O. Farkas, J. Tomasi, V. Barone, M. Cossi, R. Cammi, B. Mennucci, C. Pomelli, C. Adamo, S. Clifford, J. Ochterski, G. A. Petersson, P. Y. Ayala, Q. Cui, K. Morokuma, D. K. Malick, A. D. Rabuck, K. Raghavachari, J. B. Foresman, J. Cioslowski, J. V. Ortiz, B. B. Stefanov, G. Liu, A. Liashenko, P. Piskorz, I. Komaromi, R. Gomperts, R. L. Martin, D. J. Fox, T. Keith, M. A. Al-Laham, C. Y. Peng, A. Nanayakkara, C. Gonzalez, M. Challacombe, P. M. W. Gill, B. G. Johnson, W. Chen, M. W. Wong, J. L. Andres, M. Head-Gordon, E. S. Replogle and J. A. Pople, GAUSSIAN 98 (Revision A.7), Gaussian, Inc., Pittsburgh, PA, 1998.
- Spartan '02, Wavefunction, Inc. Irvine, CA.